HHS Public Access

Author manuscript

Alcohol Clin Exp Res. Author manuscript; available in PMC 2017 February 01.

Published in final edited form as:

Alcohol Clin Exp Res. 2016 February ; 40(2): 335–347. doi:10.1111/acer.12943.

The Circadian *Clock* Mutation Promotes Intestinal Dysbiosis

Robin M. Voigt, Ph.D.[1], **Keith C. Summa, Ph.D.**[2], **Christopher B. Forsyth, Ph.D.**[1,3], **Stefan J. Green, Ph.D.**[4,5], **Phillip Engen, B.S.**[1], **Ankur Naqib, M.S.**[4], **Martha H. Vitaterna, Ph.D.**[2], **Fred W Turek, Ph.D.**[2], and **Ali Keshavarzian, M.D.**[1,6,7]

[1]Department of Internal Medicine, Division of Gastroenterology, Rush University Medical Center, Chicago, Illinois, USA [2]Center for Sleep and Circadian Biology, Department of Neurobiology, Northwestern University, Evanston, Illinois, USA [3]Department of Biochemistry, Rush University Medical Center, Chicago, Illinois, USA [4]DNA Services Facility, Research Resources Center, University of Illinois at Chicago, Chicago, Illinois, USA [5]Department of Biological Sciences, University of Illinois at Chicago, Chicago, Illinois, USA [6]Department of Pharmacology, Rush University Medical Center, Chicago, Illinois, USA [7]Division of Pharmacology, Utrecht Institute for Pharmaceutical Sciences, Utrecht University, Utrecht, Netherlands

Abstract

Background—Circadian rhythm disruption is a prevalent feature of modern day society that is associated with an increase in pro-inflammatory diseases and there is a clear need for a better understanding of the mechanism(s) underlying this phenomenon. We have previously demonstrated that both environmental and genetic circadian rhythm disruption causes intestinal hyperpermeability and exacerbates alcohol-induced intestinal hyperpermeability and liver pathology. The intestinal microbiota can influence intestinal barrier integrity and impact immune system function; thus, in the current study, we sought to determine if genetic alteration of the core circadian clock gene, *Clock*, altered the intestinal microbiota community.

Methods—Male $Clock^{\Delta 19}$ mutant mice (mice homozygous for a dominant-negative mutant allele) or littermate wild-type mice were fed one of three experimental diets: (1) a standard chow diet, (2) an alcohol-containing diet, or (3) an alcohol-control diet in which the alcohol calories were replaced with dextrose. Stool microbiota was assessed with 16S ribosomal RNA gene amplicon sequencing.

Results—The fecal microbial community of *Clock* mutant mice had lower taxonomic diversity, relative to wild type mice and the $Clock^{\Delta 19}$ mutation was associated with intestinal dysbiosis when mice were fed either the alcohol-containing or the control diet. We found that alcohol consumption significantly altered the intestinal microbiota in both wild type and *Clock* mutant mice.

Conclusion—Our data support a model by which circadian rhythm disruption by the $Clock^{\Delta 19}$ mutation perturbs normal intestinal microbial communities and this trend was exacerbated in the context of a secondary dietary intestinal stressor.

Corresponding Author: Robin M Voigt-Zuwala, Ph.D., 1735 W Harrison St, Suite 206 Chicago IL 60612, 312-942-8973 robinmvoigt@rush.edu.

Keywords

clock mutation; circadian rhythm disruption; stool microbiota; dysbiosis; alcohol

Introduction

Circadian rhythms regulate nearly every aspect of our lives including behavior, biological systems, organ function, cellular, and molecular processes. Disruption of these rhythms can negatively impact health and immune system function which may contribute to the development or progression of inflammatory-mediated diseases following circadian rhythm disruption (Castanon-Cervantes et al., 2010; Cermakian et al., 2013). One important mechanism that may contribute to immune system dysfunction following the disruption of normal circadian rhythmicity is through effects on the intestinal microbiota.

The intestinal microbiota regulates physiological processes and it is becoming clear that disruption of the normal intestinal flora (i.e., intestinal dysbiosis) is associated with numerous diseases that are promoted or exacerbated by inflammation (Albenberg and Wu, 2014; Chan et al., 2013; Hollister et al., 2014; Kamada and Nunez, 2014). The intestinal microbiota shares a symbiotic relationship with the host whereby the host supplies food sources for the microbiota and the microbiota produce byproducts that can benefit the host. For example, short chain fatty acids (SCFA) produced by certain bacteria can fortify intestinal barrier integrity (Macia et al., 2012; Viladomiu et al., 2013) and a reduction in these SCFA-producing bacteria can negatively impact barrier integrity, thereby allowing pro-inflammatory bacteria products (e.g., lipopolysaccharide (LPS)) to pass into the systemic circulation where they can cause and promote inflammation-mediated diseases. Recent studies also show that microbial products, especially SCFA, are critical for maintaining normal mucosal immune function (Arpaia et al., 2013; Ivanov and Honda, 2012; Smith et al., 2013).

We have shown that circadian rhythm disruption induced by repeated changes in the 24h light:dark cycle (i.e., environmental disruption) or *Clock*$^{\Delta 19}$ mutation-induced changes in the molecular circadian clock (i.e., genetic disruption) promotes intestinal hyperpermeability and markedly exacerbates alcohol-induced intestinal leakiness, endotoxemia, inflammation, and hepatic pathology (Summa et al., 2013). Although it is known that alcohol changes the intestinal microbiota, the consequence of altered circadian organization on the composition and structure of the intestinal microbiota is relatively unknown. We recently demonstrated that environmental circadian rhythm disruption causes intestinal dysbiosis when combined with a high-fat, high-sugar diet (Voigt et al., 2014) and others have shown that perturbation of normal circadian rhythms in the host can impact the intestinal microbiota (Leone et al., 2015; Thaiss et al., 2014). In the current study, we expanded these findings and investigated the consequence of genetic circadian rhythm disruption, achieved via mutation of the *Clock* gene, on the intestinal microbiota and also evaluated how circadian rhythm disruption may impact alcohol-induced dysbiosis.

Materials and Methods

Animals and Experimental Protocol

Mice homozygous for the dominant negative Δ19 allele of the *Clock* gene (*Clock*$^{\Delta 19}$ mutant) were used to study genetic disruption of circadian rhythms (Antoch et al., 1997; King et al., 1997; Vitaterna et al., 1994) and wild-type littermates were used as controls. The mutation was induced in C57BL/6J mice; thus, all mice were coisogenic C57BL/6J. *Clock* mutant mice have a mutation in the canonical circadian regulatory gene, *Clock*, which impacts the period, precision, and persistence of circadian rhythms at the molecular, cellular, tissue, and behavioral levels (Herzog et al., 1998; Miller et al., 2007; Vitaterna et al., 2006). This model has been well-validated and widely used to explore the link between circadian rhythms and a variety of biological processes (McClung, 2007; Naylor et al., 2000; Turek et al., 2005).

Briefly, young adult (7–9 week old) male mice of each genotype were individually housed on a 12 hour light:12 hour dark light cycle (i.e., 12:12 LD) and fed a standard rodent chow diet (Harlan Teklad Global; Madison, WI) and subsequently placed in either the alcohol-containing or the alcohol-control experimental group. The alcohol diet is comprised of 29% of total daily calories from alcohol (4.5% v/v) and the control group received an isocaloric, alcohol-free diet with the alcohol calories being replaced with dextrose. This diet is a modification of the Leiber-Dicarli diet that has been widely used to study alcohol-induced effects on the liver. The diet is prepared fresh daily and provided to mice in a specialized feeding tube that allows for daily monitoring of food intake. There is a two-week introduction to alcohol (i.e., an alcohol ramp, 3–29% of daily calories from alcohol), followed by eight weeks on the alcohol diet (29% of daily calories from alcohol, 4.5% v/v). Mice were weighed bi-weekly and food consumption was noted daily. It is well-established that Clock mutant mice have metabolic abnormalities Laposky et al, 2008; Turek et al, 2005) and in our study *Clock* mutant mice did weigh more (significant effect of genotype, $p<0.00$) and tended to consume more food on a daily basis (significant effect of genotype, $p=0.01$) than their wild-type counterparts. However, when food consumption was normalized to body weight there was no effect of genotype on food consumption in control-fed or alcohol-fed mice ($p>0.05$, Supplemental Fig 1).

Stool samples were collected after two weeks on the standard rodent chow diet (Fig. 1A) or after ten weeks of an alcohol-containing diet or the alcohol-control diet (Fig. 1B). Stool samples were collected from each mouse over a five hour period (ZT0-ZT5, ZT0=lights on) during a test to assess intestinal barrier integrity (see Methods section below, Correlation Analysis-Intestinal Barrier Integrity). Stool samples were then subsequently frozen and stored at −80°C until use. These samples were then used in sequencing for determination of intestinal microbial community composition.

Mice were euthanized by conscious decapitation. Serum collected at the time of the tissue harvest evaluated for LPS using a commercially available ELISA kit (MBS-722939; MyBioSource, San Diego, CA) according to the manufacturer's instructions. Formalin-fixed liver was stained with hematoxylin and eosin (H&E) and a blind assessment of liver steatosis was conducted by a gastrointestinal pathologist. Steatosis severity was scored as percent

hepatocyte involvement (0 = <5%, 1 = 5–33%, 2 = 34–66%, 3 = >67%), corresponding to the fraction of lipid-containing hepatocytes.

Analysis of Microbial Community Structure

Genomic DNA was extracted from mouse fecal samples (Fast DNA SPIN Kit for Soil, #116560200, MP Biomedicals; Solon, OH). PCR amplification was performed targeting bacterial small subunit (SSU or 16S) ribosomal RNA (rRNA) genes with primers Gray28F/Gray519R, as described previously (Ishak et al., 2011). Sequencing reactions were performed on a Roche 454 FLX instrument (Roche; Indianapolis, IN) with titanium reagents and procedures, a one-step PCR, and a mixture of Hot Start and Hot Star high-fidelity Taq polymerases.

Raw sequence data were imported into the software package CLC genomics workbench (v8.0; CLC Bio, Qiagen; Boston, MA). Subsequently, merged data were quality trimmed (Q15), and sequences shorter than 350 bases were removed. The remaining sequences were exported as FASTA and processed through the software package QIIME (v1.8.0) (Caporaso et al., 2010). Briefly, sequences were screened for chimeras using the usearch61 algorithm (Edgar, 2010) and putative chimeric sequences were removed from the dataset. Data were pooled, renamed, and clustered into operational taxonomic units (OTU) at 97% similarity using the usearch61 de novo OUT picking algorithm. Representative sequences from each OTU were extracted, and these sequences were classified using the “assign taxonomy” algorithm implementing the uclust algorithm, utilizing the Greengenes reference OTU build (v13_8). A biological observation matrix (BIOM);(McDonald et al., 2012) was generated at taxonomic levels from phylum to genus using the “make OTU table” algorithm. Subsequently, each sample sequence set was sub-sampled to 1,250 sequences to reduce analytical issues associated with variable library size (Gihring et al., 2012). The sub-sampled BIOMs used for statistical analysis and visualization using group-average clustering, non-metric multidimensional scaling (NMDS), analysis of similarity (ANOSIM) and similarity percentages (SIMPER) analyses, as described previously (Voigt et al., 2014). Differences in the relative abundance of individual taxa between *a priori* defined groups were tested for significance using the “group significance” algorithm, implemented within QIIME. Tests were performed using the non-parametric Kruskal-Wallis test, generating a Benjamini-Hochberg false-discovery rate (FDR) corrected p-value. Taxa with an average abundance of <1% across the entire sample set were removed from such analyses. *In silico* community functional predications were performed using the software package PICRUSt (phylogenetic investigation of communities by reconstruction of unobserved states) and significant differences in KEGG ortholog (KO) abundances between groups were identified and analyzed using the KEGG Mapper pathway search function.

Correlation Analysis

We sought to determine if intestinal dysbiosis associated with alcohol or circadian rhythm disruption was associated with changes in gene expression in the proximal colon. Tissue samples were collected one day after the stool collection (Fig. 1B). Mice were euthanized by conscious decapitation and proximal colon samples placed into RNA Later (Qiagen; Valencia, CA), frozen in liquid nitrogen, and stored at −80°C until use. Proximal colon

samples were prepared as tissue homogenates and mRNA levels were determined using a Luminex-based custom multiplex bead array. This QuantiGene 2.0 Multiplex Assay (Affymetrix; Santa Clara, CA) was used to assess the level of expression of genes of interest. Gene expression was normalized to the average of two housekeeping genes (Phosphoglycerate kinase 1 (*Pgk1*) and polymerase polypeptide A (*Polr2a*)). Thus, mice in the following groups were included in the correlation analysis: wild type alcohol-control diet, wild type alcohol diet, *Clock*$^{\Delta 19}$ mutant alcohol-control diet, and *Clock*$^{\Delta 19}$ mutant alcohol diet.

Relative RNA level for each gene was correlated with bacterial taxa that were greater than 5% of the total microbiota community at the genus level (i.e., *Lactobacillus, Clostridium, Allobaculum, Akkermansia*). P-values were false discovery rate (FDR) corrected for multiple comparisons. *In vivo* assessment of intestinal permeability was conducted as described previously (Keshavarzian et al., 2009; Shaikh et al., 2015; Summa et al., 2013). Briefly, mice were fasted for eight hours prior to the test, which was performed at ZT0 (i.e., ZT0=lights on). A 200 μL solution containing lactulose (3.2 mg), sucrose (0.45 mg), sucralose (0.45 mg) and mannitol (0.9 mg) was administered orally (i.e., gavage), and 2 mL 0.9% saline was administered subcutaneously to promote urine production. Urine was collected for five hours and intestinal barrier integrity was determined by measuring urinary sugar concentration using gas chromatography, enabling calculation of the amount of orally administered sugar excreted in the urine over five hours. Intestinal permeability was measured after eight weeks on the full alcohol concentration (i.e., 29% of total daily calories from alcohol). Thus, mice in the following groups were included in the correlation analysis: wild type alcohol-control diet, wild type alcohol diet, *Clock*$^{\Delta 19}$ mutant alcohol-control diet, and *Clock*$^{\Delta 19}$ mutant alcohol diet.

Percent urinary sugar excretion was correlated with bacterial taxa that were greater than 5% of the total microbiota community at the genus level (i.e., *Lactobacillus, Clostridium, Allobaculum, Akkermansia*). P-values were false discovery rate (FDR) corrected for multiple comparisons.

Results

Impact of the Clock$^{\Delta 19}$ Mutation - Chow-fed Mice

We have shown that environmental disruption of circadian rhythms via changes in the light:dark cycle has no impact on the community structure of the intestinal microbiota when mice are fed a standard chow diet (Voigt et al., 2014). We sought to determine if this effect was specific to environmental disruption of circadian rhythms during adult life (12 weeks) or if it would be also observed in genetically disrupted mice where circadian homeostasis has been disrupted since birth. Following two weeks maintenance on standard chow diet, fecal samples were collected from both wild type and *Clock* mutant mice, and microbial communities were characterized using Roche 454 pyrosequencing of bacterial rRNA gene amplicons (Fig. 1A). Analysis of the rRNA gene amplicons demonstrated that the gut microbiota of mice with the *Clock*$^{\Delta 19}$ mutation had lower evenness and diversity (Shannon and Simpson indices) while microbial richness was not significantly different (Fig. 2). The effects on evenness and diversity were observed at the taxonomic levels of genus, family,

order, and class (Supplementary Table 1). Similar to the environmental circadian rhythm disruption, no significant differences in community structure were observed between wild type and *Clock*$^{\Delta 19}$ mice fed the standard rodent chow diet using analysis of similarity (ANOSIM) (Table 1) or a predictive assessment of microbial community functional potential (PICRUSt) (Table 2). Although not significant, the average relative abundance of bacteria from the family *Lachnospiraceae* was higher in mutant mice (17.5–34.8%) (Fig. 3), and this shift contributed to an increase in the Firmicutes/Bacteroidetes ratio in *Clock*$^{\Delta 19}$ mice compared to the wild type mice (Supplementary Fig 2A.).

Impact of the Clock$^{\Delta 19}$ Mutation – Alcohol-Control Diet-Fed Mice

Our group has demonstrated that environmental circadian rhythm disruption significantly impacts stool microbiota composition when mice are fed an alcohol-control diet (i.e., high-fat, high-sugar diet, 36% protein, 29% carbohydrate (dextrose), and 35% fat)) (Voigt et al., 2014) and in the current study we investigated if the same was true in *Clock*$^{\Delta 19}$ mutant mice. Microbial community analyses were performed on stool samples collected following 10 weeks of alcohol-control diet feeding (Fig. 1B). Microbial community diversity (Shannon and Simpson indices) and evenness were significantly lower in *Clock*$^{\Delta 19}$ mice fed the alcohol-control diet relative to wild type mice fed the same diet (Fig. 4, Supplementary Table 1). Similarly, microbial community structure was significantly different between alcohol-control diet-fed *Clock*$^{\Delta 19}$ mice compared to wild type mice fed the alcohol-control diet, and these differences were observed at all taxonomic levels except phylum (Table 1). Although substantial shifts in individual taxa were observed between wild type and *Clock* mutant mice, these shifts were not significant when adjusted with the false-discovery rate correction nor were any differences revealed using a predicted functional analysis (PICRUSt) (Table 2). Nonetheless, alcohol-control diet-fed *Clock*$^{\Delta 19}$ mice had communities dominated by bacteria from the genus *Clostridum*, and relatively low abundance of bacteria from the genus *Allobaculum* (class Erysipelotrichi) compared to their wild type counterparts (Fig. 5). The overall changes in the community structure contributed to a slight, but not significant, increase in the Firmicutes/Bacteroidetes ratio in *Clock*$^{\Delta 19}$ mice fed the alcohol-control diet compared to wild type mice (Supplementary Fig 2B.).

Impact of the Clock$^{\Delta 19}$ Mutation - Alcohol-fed Mice

Chronic alcohol feeding significantly decreased microbiota community evenness and diversity in wild type mice but the *Clock*$^{\Delta 19}$ mutation did not further impact microbial community diversity, richness, or evenness (Fig. 4, Supplementary Table 1). However, community structure was significantly different between *Clock*$^{\Delta 19}$ mice compared to wild type mice fed the alcohol-containing diet, and these differences were observed at all taxonomic levels (Table 1). Only a single taxon was significantly altered by the *Clock*$^{\Delta 19}$ mutation in alcohol-fed mice, which was an increase in an unidentified genus within the order Clostridiales (Firmicutes, class Clostridia, $p<0.04$) (Fig. 5).

Predictive assessment of the microbial community functional potential (PICRUSt) was performed and revealed many significant differences in the predicted function of the microbial population between alcohol-fed wild type and alcohol-fed *Clock*$^{\Delta 19}$ mutant mice. These changes were dominated by a decrease in pathways including cellular processes,

environmental information processing, genetic information processing, human diseases, metabolism, organismal systems, as well as additional unclassified pathways (Table 2, Supplementary Table 2). *Clock*$^{\Delta 19}$ mice are reported to have metabolic abnormalities (Turek et al., 2005) and indeed we identified 34 metabolic pathways that were significantly decreased by the *Clock*$^{\Delta 19}$ mutation in alcohol-fed mice. Specifically, we identified a decrease in energy metabolism, metabolism of amino acids, metabolism of terpenoids and polyketides, metabolism of carbohydrates, metabolism of cofactors and vitamins, metabolism of nucleotides, and lipid metabolism. In addition, biosynthesis of other secondary metabolites, xenobiotics degradation and metabolism, glycan biosynthesis and metabolism, and enzyme families were significantly different between wild type and *Clock*$^{\Delta 19}$ mice fed an alcohol-containing diet, with the majority of these pathways exhibiting a significant decrease in the *Clock*$^{\Delta 19}$ mice compared to their wild type counterparts (Supplementary Table 2).

Impact of Alcohol

Alcohol significantly reduced evenness and diversity in wild type mice; however, this effect was not observed in *Clock*$^{\Delta 19}$ mutant mice (Fig. 4, Supplementary Table 3). Microbiota community structure was altered by alcohol in both wild type and *Clock*$^{\Delta 19}$ mice (Table 3); but, the specific changes induced by alcohol were different in each genotype (Table 4). The microbiome of alcohol-fed wild type mice had significantly higher relative abundance of bacteria from the genus *Allobaculum* and lower relative abundance of bacteria from the genus *Lactobacillus* compared to wild type mice fed the alcohol-control diet. *Clock*$^{\Delta 19}$ mutant mice fed the alcohol-containing diet demonstrated a significant reduction in bacteria in the class Clostridia compared *Clock*$^{\Delta 19}$ mutant mice fed the alcohol-control diet (Fig. 5, Table 4).

Predictive assessment of the microbial community functional potential (PICRUSt) was performed and while numerous pathways were altered by alcohol in wild type mice no pathways were significantly altered by alcohol in *Clock*$^{\Delta 19}$ mice (Table 2). Alcohol-induced changes in wild type mice were characterized by an increase in pathways including cellular processes, environmental information processing, genetic information processing, human diseases, organismal systems, metabolism, as well as additional unclassified pathways (Table 5, Supplementary Table 4). To further characterize these changes, we used PICRUSt to evaluate bacterial secretion systems and lipopolysaccharide (LPS) biosynthesis as these are factors that can influence intestinal barrier integrity and inflammation. Seven bacterial secretion systems in the general secretory pathway (i.e., sec-SRP) were more abundant in wild type alcohol-fed mice and one type IV secretion system (i.e., VirD4) was also significantly increased (Table 6). In addition, two of three pathways in lipopolysaccharide (LPS) biosynthesis were significantly upregulated in alcohol-fed mice (Table 6). Evaluation of serum LPS levels indicated there was not a significant difference between control- and alcohol-fed wild type mice (Student's *t*-test, $p>0.05$, data not shown). We have previously demonstrated that serum LPS rhythms exhibit a robust circadian pattern (Summa et al, 2013); thus, analysis of serum LPS at a single time point may have obscured between group differences.

Functional Assessment of Intestinal Microbiota on the Host

Liver tissue was collected one day following stool collection (Fig. 1). Evaluation of the liver revealed that steatosis (the fraction of lipid containing hepatocytes) was significantly increased in groups demonstrating intestinal dysbiosis (Fig. 6). Both genotype ($F_{(1,26)}$=8.21, p=0.01) and diet ($F_{(1,26)}$=19.30, p<0.00) had a significant effect on the liver pathology suggesting that intestinal dysbiosis may contribute to fatty liver associated with alcohol consumption and circadian rhythm disruption.

There is a high degree of crosstalk between the intestinal microbiota and the intestinal epithelium; thus, we sought to determine if gene expression in the proximal colon correlated with stool bacteria. Proximal colon tissue was collected one day following collection of stool samples (Fig. 1). Again, we selected those bacterial genera that were greater than 5% of the total microbiota community on the genus level (i.e., *Lactobacillus, Clostridium, Allobaculum, Akkermansia*) and correlated them with genes of interest involved in intestinal barrier integrity, oxidative stress, and inflammation in tissue collected from the proximal colon. Specifically, these included tight junction genes *claudin 4* (*Cldn4*) and *occludin* (*Ocln*) as well as oxidative stress production gene *nicotinamide adenine dinucleotide phosphate* (*NADPH*) *oxidase 1* (*Nox1*) and *hepatocyte nuclear factor 1a* (*Hnf1a). Clostridium* negatively correlated with inflammation marker *Hnf1a* and positively correlated with oxidative stress marker *Nox1* while *Akkermansia* positively correlated with *Cldn4* and *Ocln* (Fig. 7). No correlations were observed between *Lactobacillus* or *Allobaculum* and any gene of interest (Fig. 7).

The intestinal microbiota composition can influence intestinal barrier integrity which can elicit mucosal and systemic inflammation and promote/exacerbate a number of inflammation-mediated disorders; thus, we sought to determine if intestinal leakiness associated with the *Clock* mutation and/or alcohol consumption (Summa et al. 2013) correlated with any bacterial taxon. Stool was collected during the same period as a test for intestinal barrier integrity was administered (Fig. 1B). We selected those bacterial genera that were greater than 5% of the total microbiota community (i.e., *Lactobacillus, Clostridium, Allobaculum, Akkermansia*) and correlated each taxon with percent urinary sugar excretion (greater percentage of urinary sugar content indicates greater intestinal barrier dysfunction). We found that *Clostridium* negatively correlated with both mannitol (thought to be an indication of proximal/mid small intestine permeability) and sucrose excretion (thought to be a marker of stomach and duodenum permeability) but not sucralose (primarily small intestine) or lactulose (total gut but primarily large intestine) (Fig. 8). *Lactobacillus, Allobaculum, and Akkermansia* did not correlate with any serum marker of intestinal barrier integrity (Fig. 8).

Discussion

In the current study, the $Clock^{\Delta 19}$ mutation was associated with intestinal dysbiosis. Specifically, (1) $Clock^{\Delta 19}$ chow-fed mice had a significant reduction in bacterial evenness and diversity compared to WT mice fed the same diet, (2) $Clock^{\Delta 19}$ mutant mice fed the alcohol-control diet (i.e., a high-fat, high-sugar diet) had a significant reduciton in evenness and diversity as well as a significant change in community structure compared to WT

control-fed mice, and (3) alcohol-fed *Clock*$^{\Delta 19}$ mice demonstrated a signficant alteration in community structure compared to WT mice fed alcohol. These changes may have an important funcitonal relevance as we found that liver pathology was found in all groups that exhibited intestinal dysbiosis and that specific bacterial taxon significantly correlated with markers of intestinal barrier integrity and gene expression in the proximal colon.

A reduction in bacterial diversity is a feature associated with numerous pathological conditions (Mondot et al., 2013; Round and Mazmanian, 2009). Thus, it is perhaps not surprising that we observed a reduction in bacterial diversity in *Clock*$^{\Delta 19}$ mice that have a variety of physiological abnormalities including metabolic syndrome (Turek et al., 2005). It is interesting that diversity was not further impacted by alcohol consumption in *Clock*$^{\Delta 19}$ mice; however, this may represent a floor effect as both alcohol and the *Clock*$^{\Delta 19}$ mutation impact bacterial diversity. We observed signficant alterations in community structure when *Clock*$^{\Delta 19}$ mice were fed the alcohol-control or alcohol-containing diet but not when mice were fed the standard rodent chow diet. This finding is in agreement with our previous report in which we proposed a “two hit” hypothesis whereby circadian rhythm disruption by itself may prime the microbiota community (manifested as low bacterial diversity) but may not be sufficient to promote pathology while overt effects are only observed when circadian disruption is combined with a second insult (e.g., alcohol or a high-fat, high-sugar diet). Despite the significant differences in overall community structure observed in *Clock*$^{\Delta 19}$ mice, only a single bacterial taxon was signficantly altered by the mutation and this was observed in the *Clock*$^{\Delta 19}$ alcohol-fed mice; an increase in an unidentified member of the order Clostridiales (Firmicutes, class Clostridia). The fact that this is an unidentified member makes it hard to judge how this may be influencing the mouse or why the change has taken place and further investigation will be necessary to more fully understand this alteration. Evaluation of the overall community structure using PICRUSt revealed that microbial changes in stool collected from *Clock*$^{\Delta 19}$ mice were characterized by a reduction in the number of metabolic pathways. This change is highly relevant as numerous metabolic abnormalities are a feature associated with the *Clock*$^{\Delta 19}$ mutation (Turek et al., 2005). It is not clear if this change in bacterial metabolism is a cause or a result of changes in metabolism in the host as recent publications indicate that the host can influence the microbiota and vice versa (Leone et al., 2015; Thaiss et al., 2014). It is possible that the metabolic syndrome assoicated with the *Clock*$^{\Delta 19}$ mutation may be, in part, a consequence of changes in the intestinal microbiota.

Alcohol consumption has a profound and long-lasting effect on the intestinal microbiota (Bode et al., 1984; Bull-Otterson et al., 2013; Mutlu et al., 2009; Mutlu et al., 2012; Queipo-Ortuno et al., 2012; Yan et al., 2011). The specific changes vary depending on species (mouse, rat, human), sample collection site (feces, tissue), as well as alcohol consumption protocol/history. Our results in wild type mice recapitulate some previous findings in mice: a significant decrease in *Lactobacillus* (although *Lactobacillus* has also been reported to be increased in fecal samples from alcohol-fed mice), a significant decrease in Lachnospiraceae (family), and a significant increase in *Allobaculum* (Bull-Otterson et al., 2013; Yan et al., 2011). In the current study, alcohol reduced bacterial diversity in wild type mice which is in agreement with our findings in human alcoholics and alcohol-fed rats (Mutlu et al., 2009; Mutlu et al., 2012). While alcohol significantly impacted the bacterial communities in both

wild type and *Clock*$^{\Delta 19}$ mice it is interesting to note that the alcohol-induced changes in wild type and *Clock*$^{\Delta 19}$ mice were overlapping but not identical indicating that alcohol-induced effects are, at least in part, dependent on the underlying genetic background of the host. In the current study, Clostridia (class) were primarily impacted in *Clock*$^{\Delta 19}$ mutant mice while wild type mice had changes that were dominated by bacteria in the classes Erysipelotrichi and Bacilli. Evaluation of predicted microbial community function using PICRUSt revealed an increase in bacterial secretion systems and LPS biosynthesis suggesting that pathological changes associated with chronic alcohol consumption (e.g., inflammation and liver pathology) may be, in part, a consequence of changes in the intestinal microbiome. Despite the predicted upregulation of LPS biosynthesis we did not observe a significant increase in serum LPS levels. This finding may be due to a number of factors incluing the time of sample collection. We previously demonstrated that serum LPS levels exhibit a robust circadian pattern (Summa et al., 2013) which may the consequence of the time of LPS biosynthesis in the bacteria, the intestinal barrier integrity of the host, or the ability of the host immune system to respond to and eliminate serum LPS. Future studies will be necessary to evaluate these hypotheses. Alternatively, the predicted increase in LPS biosynthesis identified via PICRUSt may not have been sufficient to result in a statistically different serum LPS level.

Little is known about the relationship between circadian rhythms and the microbiota, although recent studies have demonstrated that interactions between commensal bacteria and circadian *Clock* genes help maintain intestinal homeostasis (Mukherji et al., 2013) and that circadian rhythmicity of intestinal bacteria is regulated by the host (Leone et al., 2015; Thaiss et al., 2014). We have previously demonstrated that the *Clock*$^{\Delta 19}$ mutation causes intestinal barrier dysfunction and this effect is exacerbated by alcohol consumption (Voigt et al., 2014). Intestinal barrier integrity can be influenced by the intestinal microbiota (Sharma et al., 2010); thus, we evaluated if particular bacterial taxon were influencing intestinal barrier integtrity. Correlation analysis of predominant bacterial species in the stool (>5% of the total population) with serum markers of intestinal leakiness as well as the expression of genes that can influence barrier integrity revealed two bacterial taxa that may be contributing, *Akkermansia and Clostridium. Akkermansia*, a mucolytic bacterium, positively correlated with the tight junction genes *Cldn4* and *Ocln* and indeed this finding is in agreement with previous data demonstrating that *Akkermansia mucinphila* is anti-inflammatory and beneficial for intestinal barrier integrity (Everard et al., 2013). *Clostridium* negatively correlated with markers of barrier integrity suggesting that it may exert beneficial effects on the host, although poteintially negative effects were observed including a negative correlation with *Hnf1a* gene expression (generally considered to be beneficial) and a positive correlation with *Nox1* mRNA (encodes pro-inflammatory NADPH oxidase). We have shown that alcohol consumption disrupts intestinal barrier function (Keshavarzian et al., 1999; Keshavarzian et al., 2009; Summa et al., 2013) and in the current study *Clostridium* was markedly decreased by alcohol consumption in both wild type and *Clock*$^{\Delta 19}$ mice. Furthrmore, the family Clostridiaceae (contains the genus *Clostridium*) was significantly reduced in *Clock*$^{\Delta 19}$ mice; supporting the hypothesis that *Clostridium* plays a beneficial role in promoting intestinal barrier integrity. Bacterial fermentation by Bacteroidetes and *Clostridium* can produce short chain fatty acids (SCFA) (Cummings et al.,

1987) and SCFA, especially butyrate, can influence intestinal barrier integrity (Hamer et al., 2008; Kinoshita et al., 2002; Peng et al., 2009). Thus, SCFA production is one mechanism by which *Clostridium* could have positively impacted intestinal barrier integrity, but further studies will be required to test this hypothesis.

Circadian rhythm disruption is a prevalent feature in modern day society (Golombek et al., 2013; Reddy and O'Neill, 2010) that promotes a number of inflammation-mediated diseases. Interestingly, mice harboring a mutation in the $Clock^{\Delta 19}$ gene had features that overlapped with mice subjected to envrionmental circadian rhythm disruption (i.e., changes in the light:dark cycle) (Voigt et al., 2014), suggesting that circadian rhythm disruption may be the common feature driving the dysbiotic changes in the intestinal microbiota promoting inflammation and inflammation-mediated diseases.

Our data show for the first time that the $Clock^{\Delta 19}$ mutation, which promotes circadian rhythm disruption, has a significant effect on the intestinal microbiota. These findings provide experimental evidence to support the hypothesis that circadian rhythms in the host organism may impact the intestinal microbial community; as alcohol-induced effects were different in wild type and $Clock^{\Delta 19}$ mutant mice. Incorporating this new information about effects of alcohol and circadian disruption on the intestinal microbiota opens new avenues in our thinking of alcohol-related diseases, and may have implications more broadly for diseases characterized by circadian disruption and associated changes in the microbiota. Such information is poised to play a critical role in future medical care, when personalized pictures of health and disease risk are generated and assessed in the context of individual patients. This work contributes to a growing foundation based on mechanistic understanding upon which such a future can be constructed. The functional consequences of alcohol-induced intestinal dysbiosis need to be further explored including metabolomics and measurements of short-chain fatty acids to determine how dysbiosis may impact intestinal immune homeostasis, inflammation, and intestinal barrier function.

Supplementary Material

Refer to Web version on PubMed Central for supplementary material.

Acknowledgments

Work was supported by the National Institute on Alcohol Abuse and Alcoholism of the National Institutes of Health under award number AA020216 to AK and FWT.

References

Albenberg LG, Wu GD. Diet and the intestinal microbiome: associations, functions, and implications for health and disease. Gastroenterology. 2014; 146:1564–1572. [PubMed: 24503132]

Antoch MP, Song EJ, Chang AM, Vitaterna MH, Zhao Y, Wilsbacher LD, Sangoram AM, King DP, Pinto LH, Takahashi JS. Functional identification of the mouse circadian Clock gene by transgenic BAC rescue. Cell. 1997; 89:655–667. [PubMed: 9160756]

Arpaia N, Campbell C, Fan X, Dikiy S, van der Vekken J, deRoos P, Liu H, Cross JR, Pfeffer K, Coffer PJ, Rudensky AY. Metabolites produced by commensal bacteria promote peripheral regulatory T-cell generation. Nature. 2013; 504:451–455. [PubMed: 24226773]

Bode JC, Bode C, Heidelbach R, Durr HK, Martini GA. Jejunal microflora in patients with chronic alcohol abuse. Hepatogastroenterology. 1984; 31:30–34. [PubMed: 6698486]

Bull-Otterson L, Feng W, Kirpich I, Wang Y, Qin X, Liu Y, Gobejishvili L, Joshi-Barve S, Ayvaz T, Petrosino J, Kong M, Barker D, McClain C, Barve S. Metagenomic analyses of alcohol induced pathogenic alterations in the intestinal microbiome and the effect of Lactobacillus rhamnosus GG treatment. PLoS One. 2013; 8:e53028. [PubMed: 23326376]

Caporaso JG, Kuczynski J, Stombaugh J, Bittinger K, Bushman FD, Costello EK, Fierer N, Pena AG, Goodrich JK, Gordon JI, Huttley GA, Kelley ST, Knights D, Koenig JE, Ley RE, Lozupone CA, McDonald D, Muegge BD, Pirrung M, Reeder J, Sevinsky JR, Turnbaugh PJ, Walters WA, Widmann J, Yatsunenko T, Zaneveld J, Knight R. QIIME allows analysis of high-throughput community sequencing data. Nat Methods. 2010; 7:335–336. [PubMed: 20383131]

Castanon-Cervantes O, Wu M, Ehlen JC, Paul K, Gamble KL, Johnson RL, Besing RC, Menaker M, Gewirtz AT, Davidson AJ. Dysregulation of inflammatory responses by chronic circadian disruption. J Immunol. 2010; 185:5796–5805. [PubMed: 20944004]

Cermakian N, Lange T, Golombek D, Sarkar D, Nakao A, Shibata S, Mazzoccoli G. Crosstalk between the circadian clock circuitry and the immune system. Chronobiol Int. 2013; 30:870–888. [PubMed: 23697902]

Chan YK, Estaki M, Gibson DL. Clinical consequences of diet-induced dysbiosis. Ann Nutr Metab. 2013; 63(Suppl 2):28–40. [PubMed: 24217034]

Cummings JH, Pomare EW, Branch WJ, Naylor CP, Macfarlane GT. Short chain fatty acids in human large intestine, portal, hepatic and venous blood. Gut. 1987; 28:1221–1227. [PubMed: 3678950]

Edgar RC. Search and clustering orders of magnitude faster than BLAST. Bioinformatics. 2010; 26:2460–2461. [PubMed: 20709691]

Everard A, Belzer C, Geurts L, Ouwerkerk JP, Druart C, Bindels LB, Guiot Y, Derrien M, Muccioli GG, Delzenne NM, de Vos WM, Cani PD. Cross-talk between Akkermansia muciniphila and intestinal epithelium controls diet-induced obesity. Proc Natl Acad Sci USA. 2013; 110:9066–9071. [PubMed: 23671105]

Gihring TM, Green SJ, Schadt CW. Massively parallel rRNA gene sequencing exacerbates the potential for biased community diversity comparisons due to variable library sizes. Environ Microbiol. 2012; 14:285–290. [PubMed: 21923700]

Golombek DA, Casiraghi LP, Agostino PV, Paladino N, Duhart JM, Plano SA, Chiesa JJ. The times they're a-changing: effects of circadian desynchronization on physiology and disease. J Physiol Paris. 2013; 107:310–322. [PubMed: 23545147]

Hamer HM, Jonkers D, Venema K, Vanhoutvin S, Troost FJ, Brummer RJ. Review article: the role of butyrate on colonic function. Aliment Pharmacol Ther. 2008; 27:104–119. [PubMed: 17973645]

Herzog ED, Takahashi JS, Block GD. Clock controls circadian period in isolated suprachiasmatic nucleus neurons. Nat Neurosci. 1998; 1:708–713. [PubMed: 10196587]

Hollister EB, Gao C, Versalovic J. Compositional and functional features of the gastrointestinal microbiome and their effects on human health. Gastroenterology. 2014; 146:1449–1458. [PubMed: 24486050]

Ishak HD, Plowes R, Sen R, Kellner K, Meyer E, Estrada DA, Dowd SE, Mueller UG. Bacterial diversity in Solenopsis invicta and Solenopsis geminata ant colonies characterized by 16S amplicon 454 pyrosequencing. Microb Ecol. 2011; 61:821–831. [PubMed: 21243351]

Ivanov II, Honda K. Intestinal commensal microbes as immune modulators. Cell Host Microbe. 2012; 12:496–508. [PubMed: 23084918]

Kamada N, Nunez G. Regulation of the immune system by the resident intestinal bacteria. Gastroenterology. 2014; 146:1477–1488. [PubMed: 24503128]

Keshavarzian A, Farhadi A, Forsyth CB, Rangan J, Jakate S, Shaikh M, Banan A, Fields JZ. Evidence that chronic alcohol exposure promotes intestinal oxidative stress, intestinal hyperpermeability and endotoxemia prior to development of alcoholic steatohepatitis in rats. J Hepatol. 2009; 50:538–547. [PubMed: 19155080]

Keshavarzian A, Holmes EW, Patel M, Iber F, Fields JZ, Pethkar S. Leaky gut in alcoholic cirrhosis: a possible mechanism for alcohol-induced liver damage. Am J Gastroenterol. 1999; 94:200–207. [PubMed: 9934756]

King DP, Zhao Y, Sangoram AM, Wilsbacher LD, Tanaka M, Antoch MP, Steeves TD, Vitaterna MH, Kornhauser JM, Lowrey PL, Turek FW, Takahashi JS. Positional cloning of the mouse circadian clock gene. Cell. 1997; 89:641–653. [PubMed: 9160755]

Kinoshita M, Suzuki Y, Saito Y. Butyrate reduces colonic paracellular permeability by enhancing PPARgamma activation. Biochem Biophys Res Commun. 2002; 293:827–831. [PubMed: 12054544]

Laposky A, Bass J, Kohsaka A, Turek FW. Sleep and circadian rhythms: key components in the regulation of energy metabolism. FEBS Lett. 2008; 582:142–151. [PubMed: 17707819]

Leone V, Gibbons SM, Martinez K, Hutchison AL, Huang EY, Cham CM, Pierre JF, Heneghan AF, Nadimpalli A, Hubert N, Zale E, Wang Y, Huang Y, Theriault B, Dinner AR, Musch MW, Kudsk KA, Prendergast BJ, Gilbert JA, Chang EB. Effects of diurnal variation of gut microbes and high-fat feeding on host circadian clock function and metabolism. Cell Host Microbe. 2015; 17:681–689. [PubMed: 25891358]

Liang X, Bushman FD, FitzGerald GA. Rhythmicity of the intestinal microbiota is regulated by gender and the host circadian clock. Proc Natl Acad Sci USA. 2015 Epub before print: pii:201501305.

Macia L, Thorburn AN, Binge LC, Marino E, Rogers KE, Maslowski KM, Vieira AT, Kranich J, Mackay CR. Microbial influences on epithelial integrity and immune function as a basis for inflammatory diseases. Immunol Rev. 2012; 245:164–176. [PubMed: 22168419]

McClung CA. Role for the Clock gene in bipolar disorder. Cold Spring Harb Symp Quant Biol. 2007; 72:637–644. [PubMed: 18419323]

McDonald D, Clemente JC, Kuczynski J, Rideout JR, Stombaugh J, Wendel D, Wilke A, Huse S, Hufnagle J, Meyer F, Knight R, Caporaso JG. The Biological Observation Matrix (BIOM) format or: how I learned to stop worrying and love the ome-ome. Gigascience. 2012; 1:7. [PubMed: 23587224]

Miller BH, McDearmon EL, Panda S, Hayes KR, Zhang J, Andrews JL, Antoch MP, Walker JR, Esser KA, Hogenesch JB, Takahashi JS. Circadian and CLOCK-controlled regulation of the mouse transcriptome and cell proliferation. Proc Natl Acad Sci USA. 2007; 104:3342–3347. [PubMed: 17360649]

Mondot S, de Wouters T, Dore J, Lepage P. The human gut microbiome and its dysfunctions. Dig Dis. 2013; 31:278–285. [PubMed: 24246975]

Mukherji A, Kobiita A, Ye T, Chambon P. Homeostasis in intestinal epithelium is orchestrated by the circadian clock and microbiota cues transduced by TLRs. Cell. 2013; 153:812–827. [PubMed: 23663780]

Mutlu E, Keshavarzian A, Engen P, Forsyth CB, Sikaroodi M, Gillevet P. Intestinal dysbiosis: a possible mechanism of alcohol-induced endotoxemia and alcoholic steatohepatitis in rats. Alcohol Clin Exp Res. 2009; 33:1836–1846. [PubMed: 19645728]

Mutlu EA, Gillevet PM, Rangwala H, Sikaroodi M, Naqvi A, Engen PA, Kwasny M, Lau CK, Keshavarzian A. Colonic microbiome is altered in alcoholism. Am J Physiol Gastrointest Liver Physiol. 2012; 302:G966–G978. [PubMed: 22241860]

Naylor E, Bergmann BM, Krauski K, Zee PC, Takahashi JS, Vitaterna MH, Turek FW. The circadian clock mutation alters sleep homeostasis in the mouse. J Neurosci. 2000; 20:8138–8143. [PubMed: 11050136]

Peng L, Li ZR, Green RS, Holzman IR, Lin J. Butyrate enhances the intestinal barrier by facilitating tight junction assembly via activation of AMP-activated protein kinase in Caco-2 cell monolayers. J Nutr. 2009; 139:1619–1625. [PubMed: 19625695]

Queipo-Ortuno MI, Boto-Ordonez M, Murri M, Gomez-Zumaquero JM, Clemente-Postigo M, Estruch R, Cardona DF, Andres-Lacueva C, Tinahones FJ. Influence of red wine polyphenols and ethanol on the gut microbiota ecology and biochemical biomarkers. Am J Clin Nutr. 2012; 95:1323–1334. [PubMed: 22552027]

Reddy AB, O'Neill JS. Healthy clocks, healthy body, healthy mind. Trends Cell Biol. 2010; 20:36–44. [PubMed: 19926479]

Round JL, Mazmanian SK. The gut microbiota shapes intestinal immune responses during health and disease. Nat Rev Immunol. 2009; 9:313–323. [PubMed: 19343057]

Shaikh M, Rajan K, Forsyth CB, Voigt RM, Keshavarzian A. Simultaneous gas-chromatographic urinary measurement of sugar probes to assess intestinal permeability: use of time course analysis to optimize its use to assess regional gut permeability. Clin Chim Acta. 2015; 442:24–32. [PubMed: 25591964]

Sharma R, Young C, Neu J. Molecular modulation of intestinal epithelial barrier: contribution of microbiota. J Biomed Biotechnol. 2010; 2010:305879. [PubMed: 20150966]

Smith PM, Howitt MR, Panikov N, Michaud M, Gallini CA, Bohlooly Y, Glickman JN, Garrett WS. The microbial metabolites, short-chain fatty acids, regulate colonic Treg cell homeostasis. Science. 2013; 341:569–573. [PubMed: 23828891]

Summa KC, Voigt RM, Forsyth CB, Shaikh M, Cavanaugh K, Tang Y, Vitaterna MH, Song S, Turek FW, Keshavarzian A. Disruption of the Circadian Clock in Mice Increases Intestinal Permeability and Promotes Alcohol-Induced Hepatic Pathology and Inflammation. PLOS One. 2013; 8:e67102. [PubMed: 23825629]

Thaiss CA, Zeevi D, Levy M, Zilberman-Schapira G, Suez J, Tengeler AC, Abramson L, Katz MN, Korem T, Zmora N, Kuperman Y, Biton I, Gilad S, Harmelin A, Shapiro H, Halpern Z, Segal E, Elinav E. Transkingdom control of microbiota diurnal oscillations promotes metabolic homeostasis. Cell. 2014; 159:514–529. [PubMed: 25417104]

Turek FW, Joshu C, Kohsaka A, Lin E, Ivanova G, McDearmon E, Laposky A, Losee-Olson S, Easton A, Jensen DR, Eckel RH, Takahashi JS, Bass J. Obesity and metabolic syndrome in circadian Clock mutant mice. Science. 2005; 308:1043–1045. [PubMed: 15845877]

Viladomiu M, Hontecillas R, Yuan L, Lu P, Bassaganya-Riera J. Nutritional protective mechanisms against gut inflammation. J Nutr Biochem. 2013; 24:929–939. [PubMed: 23541470]

Vitaterna MH, King DP, Chang AM, Kornhauser JM, Lowrey PL, McDonald JD, Dove WF, Pinto LH, Turek FW, Takahashi JS. Mutagenesis and mapping of a mouse gene, Clock, essential for circadian behavior. Science. 1994; 264:719–725. [PubMed: 8171325]

Vitaterna MH, Ko CH, Chang AM, Buhr ED, Fruechte EM, Schook A, Antoch MP, Turek FW, Takahashi JS. The mouse Clock mutation reduces circadian pacemaker amplitude and enhances efficacy of resetting stimuli and phase-response curve amplitude. Proc Natl Acad Sci USA. 2006; 103:9327–9332. [PubMed: 16754844]

Voigt RM, Forsyth CB, Green SJ, Mutlu E, Engen P, Vitaterna MH, Turek FW, Keshavarzian A. Circadian disorganization alters intestinal microbiota. PLOS One. 2014; 9:e97500. [PubMed: 24848969]

Yan AW, Fouts DE, Brandl J, Starkel P, Torralba M, Schott E, Tsukamoto H, Nelson KE, Brenner DA, Schnabl B. Enteric dysbiosis associated with a mouse model of alcoholic liver disease. Hepatology. 2011; 53:96–105. [PubMed: 21254165]

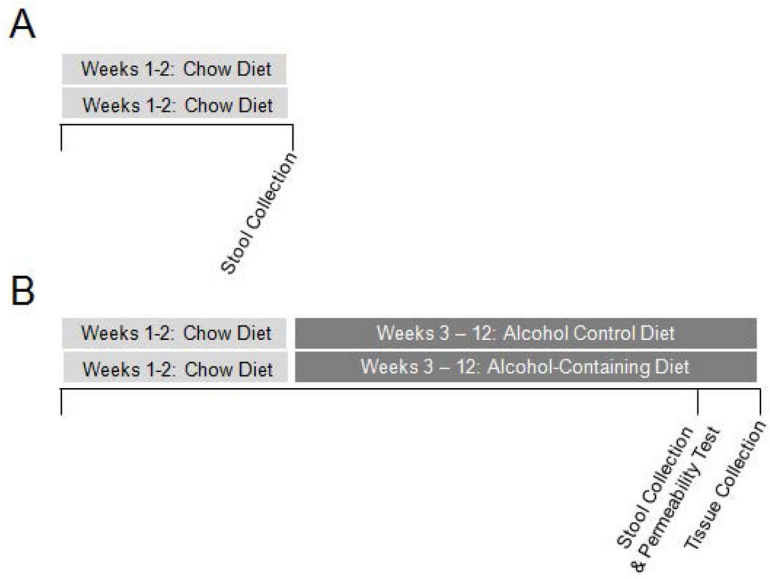

Figure 1.

Experimental Protocol. Young adult (7–9 week) male *Clock*$^{\Delta 19}$ mutant mice and wild type littermates (C57BL/6J) were housed individually and maintained on a 12 hour light:12 hour dark light cycle (i.e., 12:12 LD). (**A**) Mice were fed the standard chow (Harlan Teklad Global) and stool was collected two weeks later for analysis. Mice were placed in a metabolic chamber and stool was collected for five hours (ZT0-ZT5). (**B**) Mice were fed standard rodent chow for the first two weeks of the study then fed either an alcohol-control diet or an alcohol-containing diet (two weeks of a gradual increase in alcohol concentration, followed by eight weeks at the full alcohol dose, 29% of total daily calories from alcohol (4.5% v/v)) for 10 weeks. Mice were placed into a metabolic chamber for five hours (ZT0-ZT5) and urine and stool were collected for analysis of intestinal barrier integrity and stool microbiota analysis, respectively. One day later mice were euthanized at ZT6 and proximal colon tissue was collected for analysis.

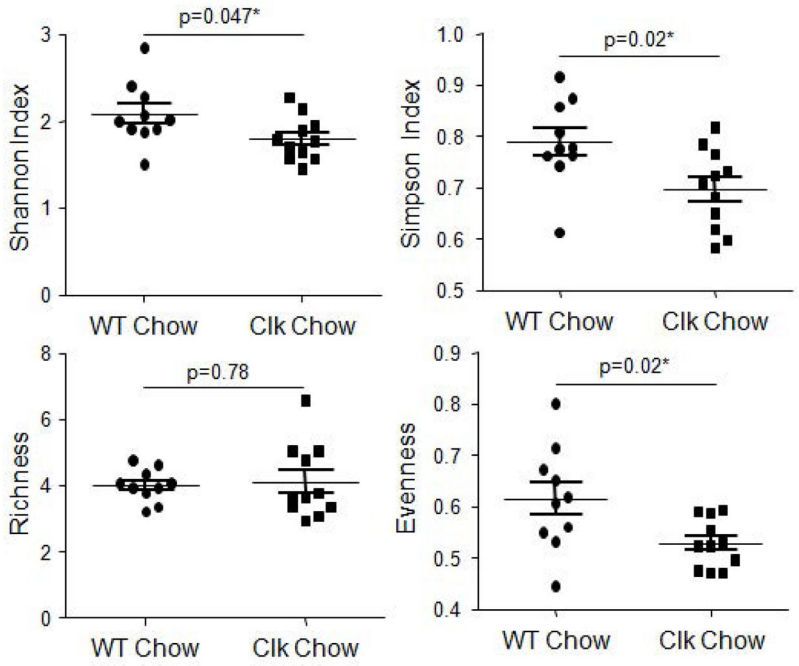

Figure 2.

The *Clock*$^{\Delta 19}$ mutation reduces bacterial diversity and evenness. Stool was collected from wild type (n=10) and *Clock*$^{\Delta 19}$ mutant mice (n=10) fed a standard rodent diet (Harlan Teklad Global) for two weeks and the stool was characterized using Roche 454 pyrosequencing of bacterial rRNA gene amplicons. Analysis of the rRNA gene amplicons was used to compare bacterial diversity (Shannon and Simpson indices), richness, and evenness. Genus level comparisons are shown (mean ± standard error of the mean (SEM)) and p-values indicate between group analyses using a Student's *t*-test followed by a false discovery rate correction for multiple comparisons. WT, wild type; Clk, *Clock*$^{\Delta 19}$ mutant mice; Chow, standard rodent chow diet.

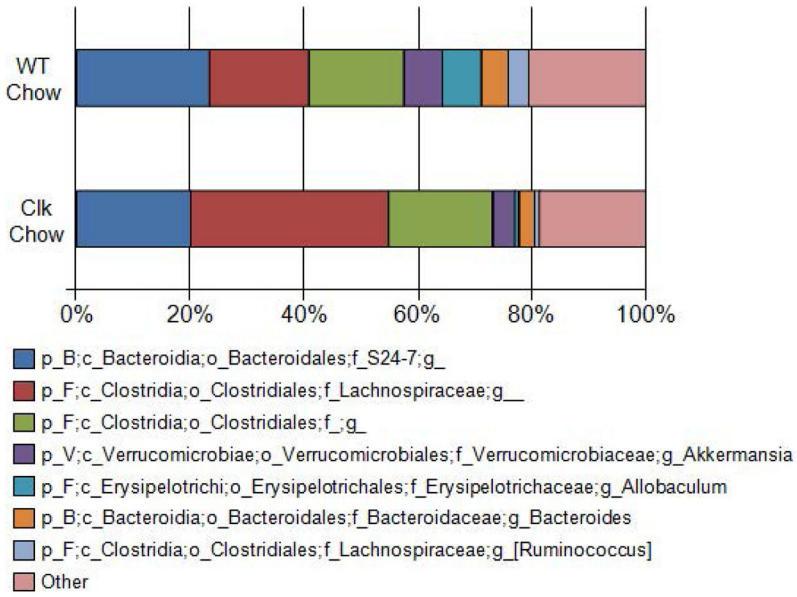

Genus	% Average Abundance	
	WT Chow	Clk Chow
p_B;c_Bacteroidia;f_S24-7;g_	23.4	20.0
p_F;c_Clostridia;f_Lachnospiraceae;g_	17.5	34.8
p_F;c_Clostridia;f_;g_	16.7	18.3
p_V;c_Verrucomicrobiae;f_Verrucomicrobiaceae;g_Akkermansia	6.8	3.8
p_F;c_Erysipelotrichi;f_Erysipelotrichaceae;g_Allobaculum	6.7	0.6
p_B;c_Bacteroidia;f_Bacteroidaceae;g_Bacteroides	4.7	2.7
p_F;c_Clostridia;f_Lachnospiraceae;g_[Ruminococcus]	3.8	1.1
p_B;c_Bacteroidia;f_Porphyromonadaceae;g_Parabacteroides	2.7	3.0
p_P;c_Epsilonproteobacteria;f_Heliobacteraceae;Other	1.9	1.4
p_B;c_Bacteroidia;f_Prevotellaceae;g_Prevotella	1.8	1.0
p_P;c_Alphaproteobacteria;f_;g_	1.1	0.6
p_F;c_Clostridia;f_Ruminococcaceae;g_Oscillospira	1.0	1.3
Other	12.0	11.3

Figure 3.

Percent average abundance of the most abundant taxon for wild type and *Clock*$^{\Delta 19}$ mice fed a standard rodent chow diet. Stool was collected from wild type (n=10) and *Clock*$^{\Delta 19}$ mutant mice (n=10) fed a standard rodent diet (Harlan Teklad Global) for two weeks and the stool was characterized using Roche 454 pyrosequencing of bacterial rRNA gene amplicons. The bar graph graphically represents and the table summarizes the average relative abundance of classified bacterial SSU rRNA gene amplicons belonging to the most abundant taxon at the genus level. WT, wild type mice; Clk, *Clock*$^{\Delta 19}$ mutant mice; Chow, standard rodent chow diet; p_, phylum; c_, class; o_, order; f_, family; g_, genus; B, Bacteroidetes; F, Firmicutes; P, Proteobacteria; V, Verrucomicrobia.

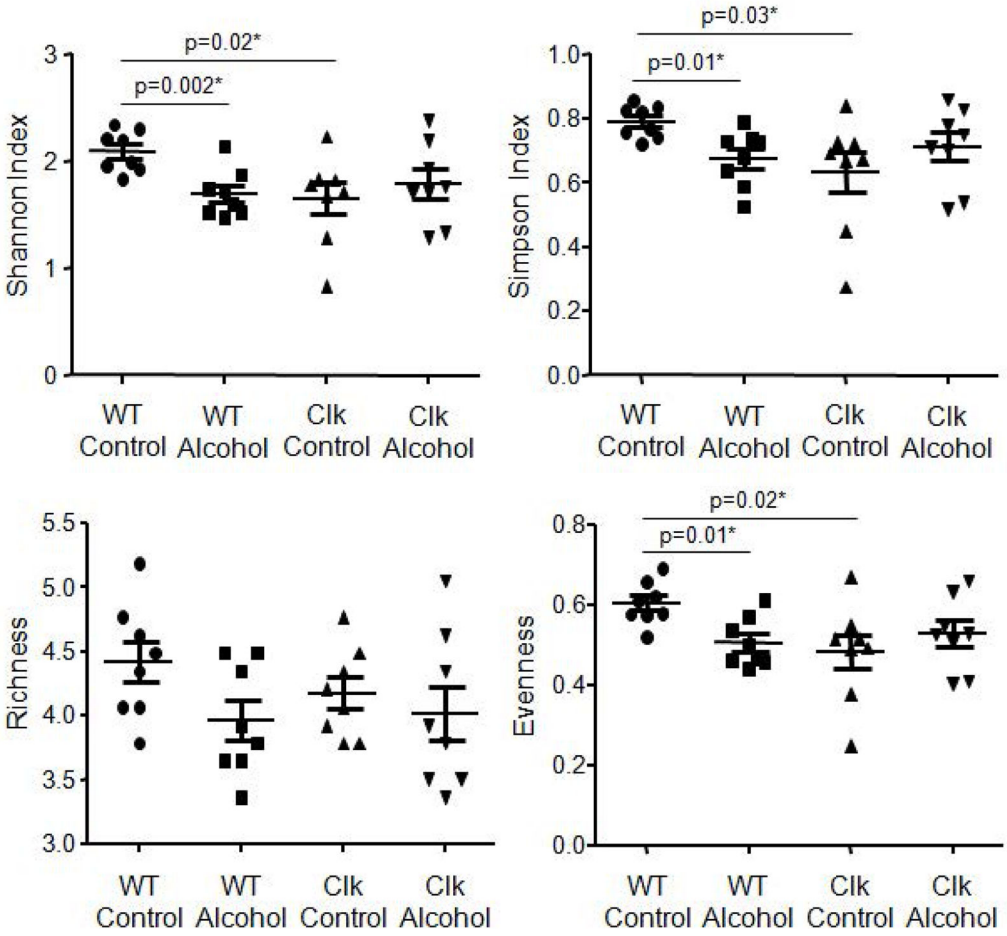

Figure 4.

The *Clock*$^{\Delta 19}$ mutation and alcohol consumption reduce bacterial diversity and evenness. Stool was collected from wild type and *Clock*$^{\Delta 19}$ mutant mice fed a standard rodent diet (Harlan Teklad Global) for two weeks followed by 10 weeks on an alcohol-control (wild type n=8, *Clock*$^{\Delta 19}$ mutant n=8) or an alcohol-containing (wild type n=8, *Clock*$^{\Delta 19}$ mutant n=8) experimental diet and the stool was characterized using Roche 454 pyrosequencing of bacterial rRNA gene amplicons. Analysis of the rRNA gene amplicons was used to compare bacterial diversity (Shannon and Simpson indices), richness, and evenness. Genus level comparisons are shown (mean ± standard error of the mean (SEM)) and p-values indicate between group analyses using a Student's *t*-test followed by a false discovery rate correction for multiple comparisons. WT, wild type; Clk, *Clock*$^{\Delta 19}$ mutant mice; Chow, standard rodent diet. WT, wild type mice; Clk, *Clock*$^{\Delta 19}$ mutant mice; Control, alcohol-control diet; Alcohol, alcohol-containing diet.

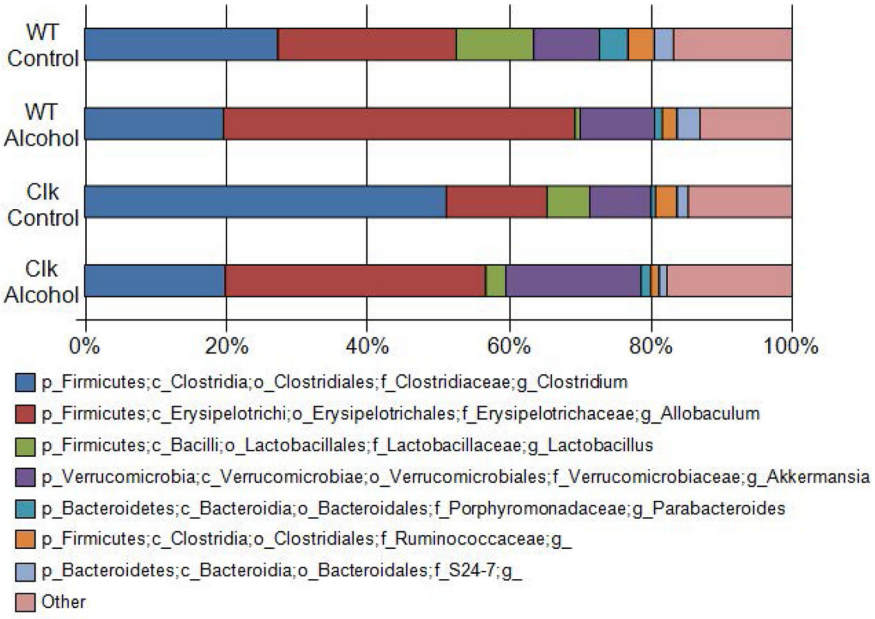

Genus	% Average Abundance			
	WT Control	WT Alcohol	Clk Control	Clk Alcohol
p_F;c_Clostridia;f_Clostridiaceae;g_Clostridium	27.3	19.6	51.0	19.8
p_F;c_Erysipelotrichi;f_Erysipelorichaceae;g_Allobaculum	25.1	49.7	14.4	36.9
p_F;c_Bacilli;f_Lactobacillaceae;g_Lactobacillus	11.1	0.7	6.0	2.8
p_V;c_Verrucomicrobiae;f_Verrucomicrobiaceae;g_Akkermansia	9.3	10.4	8.6	19.2
p_B;c_Bacteroidia;f_Porphyromonadaceae;g_Parabacteroides	4.1	1.1	0.8	1.3
p_F;c_Clostridia;f_Ruminococcaceae;g_	3.7	2.2	3.0	1.1
p_B;c_Bacteroidia;f_S24-7;g_	2.9	3.3	1.6	1.4
p_B;c_Bacteroidia;f_Bacteroidaceae;g_Bacteroides	2.4	1.8	2.0	2.1
p_P;c_Betaproteobacteria;f_Alcaligenaceae;g_Sutterella	1.5	0.5	0.3	0.6
p_F;c_Clostridia;f_;g_	1.3	1.6	3.5	1.5
p_A;c_Coriobacteriia;f_Coriobacteriaceae;g_	1.2	1.4	0.3	0.4
p_F;c_Clostridia;Other;Other	0.6	0.7	1.5	3.0*
p_F;c_Clostridia;f_Lachnospiraceae;g_	0.9	0.5	0.8	1.0
p_P;c_Gammaproteobacteria;f_Enterobacteriaceae;g_	0.6	1.0	0.2	1.7
p_F;c_Bacilli;f_Enterococcaceae;g_Enterococcus	0.1	0.1	0	1.7
Other	8.3	5.3	6.1	6.0

Figure 5.

Percent average abundance of the most abundant taxon for wild type and *Clock*$^{\Delta 19}$ mice fed either an alcohol-control diet or an alcohol-containing diet. Stool was collected from wild type and *Clock*$^{\Delta 19}$ mutant mice fed a standard rodent diet (Harlan Teklad Global) for two weeks followed by 10 weeks on an alcohol-control (wild type n=8, *Clock*$^{\Delta 19}$ mutant n=8) or an alcohol-containing (wild type n=8, *Clock*$^{\Delta 19}$ mutant n=8) experimental diet. Stool was characterized using Roche 454 pyrosequencing of bacterial rRNA gene amplicons. The bar graph graphically represents and the table summarizes the average relative abundance of classified bacterial SSU rRNA gene amplicons belonging to the most abundant taxon at the genus level. WT, wild type mice; Clk, *Clock*$^{\Delta 19}$ mutant mice; Control, alcohol-control diet; Alcohol, alcohol-containing diet; p_, phylum, c_, class; o_, order; f_, family, g_genus; A, Actinobacteria; B, Bacteroidetes; F, Firmicutes; P, Proteobacteria; V, Verrucomicrobia.

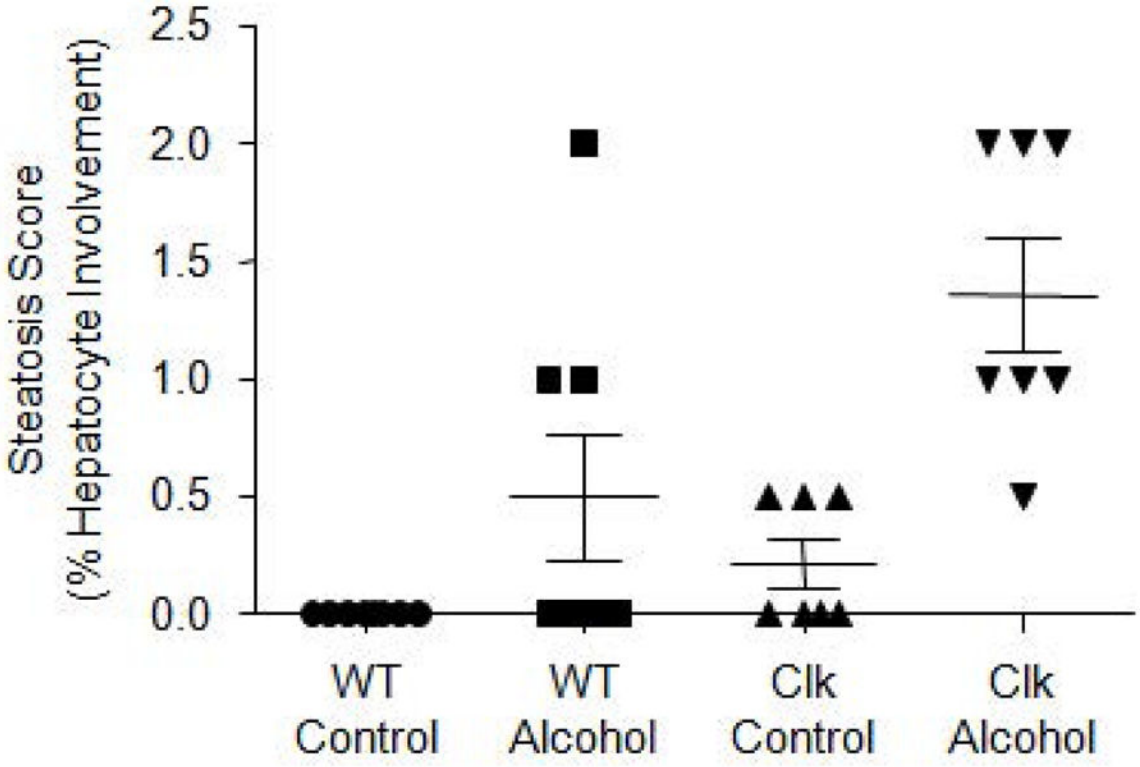

Figure 6.

Liver steatosis is observed in groups demonstrating intestinal dysbiosis. Formalin-fixed liver was stained with hematoxylin and eosin (H&E) steatosis severity was scored as percent hepatocyte involvement (0 = <5%, 1 = 5–33%, 2 = 34–66%, 3 = >67%), corresponding to the fraction of lipid-containing hepatocytes. Data were analyzed via two-way ANOVA and shown as mean±standard error of the mean. WT, wild type mice; Clk, *Clock*$^{\Delta 19}$ mutant mice; Control, alcohol-control diet; Alcohol, alcohol-containing diet.

Genus	*Cldn4* R, R^2, P-Value	*Ocln* R, R^2, P-Value	*Nox1* R, R^2, P-Value	*Hnf1a* R, R^2, P-Value
Lactobacillus	-0.12, 0.01, 0.85	-0.16, 0.02, 0.60	-0.10, 0.01, 0.75	0.03, <0.00, 0.91
Clostridium	-0.17, 0.03, 0.85	-0.36, 0.13, 0.37	0.66, 0.44, <0.00*	-0.65, 0.42, <0.00*
Allobaculum	0.06, <0.00, 0.85	0.20, 0.04, 0.54	-0.46, 0.22, 0.12	0.39, 0.15, 0.16
Akkermansia	0.56, 0.31, 0.04*	0.57, 0.33, 0.04*	-0.25, 0.07, 0.46	0.46, 0.21, 0.11

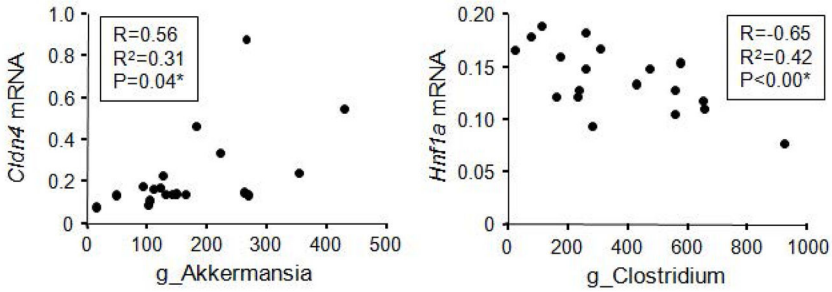

Figure 7.

Clostridium and *Akkermansia* correlate with proximal colon markers of intestinal barrier integrity and inflammation. Stool and proximal colon tissue were collected from wild type and *Clock*$^{\Delta 19}$ mutant mice fed a standard rodent diet (Harlan Teklad Global) for two weeks followed by 10 weeks on an alcohol-control (wild type n=8, *Clock*$^{\Delta 19}$ mutant n=8) or an alcohol-containing (wild type n=8, *Clock*$^{\Delta 19}$ mutant n=8) experimental diet. Stool microbial communities were characterized using Roche 454 pyrosequencing of bacterial rRNA gene amplicons and proximal colon tissue was analyzed for mRNA expression of genes of interest using an Affymetrix luminex based gene array. Genes included: *Cldn4*, claudin 4 (tight junction); *Ocln*, occludin (tight junction); *Nox1*, nicotinamide adenine dinucleotide phosphase (NAPDPH) oxidase (oxidative stress); *Hnf1a*, hypoxia inducible factor 1a (inflammation). Bacterial genera that were greater than 5% of the total microbiota community were correlated with mRNA expression (Pearson correlation) and p-values were false discovery rate corrected for multiple comparisons. g_, genus.

Genus	Mannitol (R, R^2, P-Value)	Sucralose (R, R^2, P-Value)	Lactulose (R, R^2, P-Value)	Sucrose (R, R^2, P-Value)
Lactobacillus	-0.07, 0.01, 0.78	-0.20, 0.04, 0.46	-0.07, <0.00, 0.80	0.04, <0.00, 0.89
Clostridium	-0.65, 0.42, 0.04*	-0.51, 0.26, 0.16	-0.58, 0.33, 0.08	-0.62, 0.38, 0.04*
Allobaculum	0.44, 0.19, 0.18	0.31, 0.10, 0.32	0.37, 0.14, 0.32	0.29, 0.09, 0.36
Akkermansia	0.17, 0.03, 0.71	0.45, 0.20, 0.16	0.11, 0.01, 0.80	0.43, 0.19, 0.18

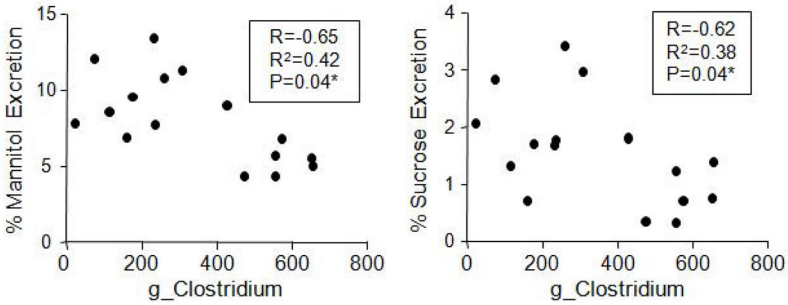

Figure 8.

Clostridium correlates with markers of intestinal hyperpermeability. Stool and urine were collected from wild type and *Clock*$^{\Delta 19}$ mutant mice fed a standard rodent diet (Harlan Teklad Global) for two weeks followed by 10 weeks on an alcohol-control (wild type n=8, *Clock*$^{\Delta 19}$ mutant n=8) or an alcohol-containing (wild type n=8, *Clock*$^{\Delta 19}$ mutant n=8) experimental diet. Stool microbial communities were characterized using Roche 454 pyrosequencing of bacterial rRNA gene amplicons and urine was analyzed for urinary sugar content following a gavage of non-digestible, non-absorbable sugars (mannitol, sucralose, lactulose, sucrose). Bacterial genera that were greater than 5% of the total microbiota community were correlated with percent urinary urinary sugar excretion (Pearson correlation) and p-values were false discovery rate corrected for multiple comparisons. g_, genus.

Table 1

Mutation of the *Clock*$^{\Delta 19}$ gene impacts stool microbiota community structure when mice were fed an alcohol-control diet (i.e., high-fat, high-sugar) or an alcohol-containing diet. Bray-Curtis metric was calculated in a pair-wise fashion and analysis of similarity (ANOSIM) was performed. Global R is based on ANOSIM analysis. P-values are calculated based on a permutations analysis, employing 999 permutations and p –values were false discovery rate corrected for multiple comparisons. WT, wild type mice, *Clock*$^{\Delta 19}$ mutant mice; Chow, standard rodent chow diet; Control, alcohol-control diet (i.e., high-fat, high-sugar diet); Alcohol, alcohol-containing diet.

		Taxonomic level	Global R	p-value
Standard Chow Diet				
WT Chow (n=10)	*Clock*$^{\Delta 19}$ Chow (n=10)	Phylum	0.04	0.24
		Class	0.04	0.24
		Order	0.03	0.26
		Family	0.01	0.28
		Genus	0.01	0.30
Alcohol Control Diet				
WT Control (n=8)	*Clock*$^{\Delta 19}$ Control (n=8)	Phylum	0.10	0.13
		Class	0.22	0.03*
		Order	0.22	0.03*
		Family	0.24	0.02*
		Genus	0.21	0.02*
Alcohol Diet				
WT Alcohol (n=8)	*Clock*$^{\Delta 19}$ Alcohol (n=8)	Phylum	0.21	0.01*
		Class	0.22	0.01*
		Order	0.22	0.02*
		Family	0.25	0.01*
		Genus	0.30	<0.00*

Table 2

The *Clock*$^{\Delta 19}$ mutation significantly impacts KEGG ortholog abundances in alcohol-fed mice. KEGG ortholog abundance was compared between groups using a Student's *t*-test and p-values were false discovery rate corrected for multiple comparisons. The number of significant between group differences was tabulated for each KEGG ortholog category. WT, wild type mice; Clk, *Clock*$^{\Delta 19}$ mutant mice; Chow, standard rodent chow diet; Control, alcohol-control diet (i.e., high-fat, high-sugar diet); Alcohol, alcohol-containing diet.

		WT Chow v Clk Chow	WT Control v Clk Control	WT Alcohol v Clk Alcohol
Cellular Processes	Pathways Increased (%)	0 (0)	0 (0)	0 (0)
	Pathways Decreased (%)	0 (0)	0 (0)	2 (20)
Environmental Information Processing	Pathways Increased (%)	0 (0)	0 (0)	0 (0)
	Pathways Decreased (%)	0 (0)	0 (0)	2 (15)
Genetic Information Processing	Pathways Increased (%)	0 (0)	0 (0)	0 (0)
	Pathways Decreased (%)	0 (0)	0 (0)	17 (65)
Human Diseases	Pathways Increased (%)	0 (0)	0 (0)	0 (0)
	Pathways Decreased (%)	0 (0)	0 (0)	9 (29)
Metabolism	Pathways Increased (%)	0 (0)	0 (0)	0 (0)
	Pathways Decreased (%)	0 (0)	0 (0)	34 (25)
Organismal Systems	Pathways Increased (%)	0 (0)	0 (0)	0 (0)
	Pathways Decreased (%)	0 (0)	0 (0)	5 (28)
Unclassified	Pathways Increased (%)	0 (0)	0 (0)	0 (0)
	Pathways Decreased (%)	0 (0)	0 (0)	6 (22)

Table 3

Alcohol impacts stool microbiota community structure in both wild type and *Clock*$^{\Delta 19}$ mutant mice. Bray-Curtis metric was calculated in a pair-wise fashion and analysis of similarity (ANOSIM) was performed. Global R is based on ANOSIM analysis. P-values are calculated based on a permutations analysis, employing 999 permutations and p-values were false discovery rate corrected for multiple comparisons. WT, wild type mice, *Clock*$^{\Delta 19}$ mutant mice; Control, alcohol-control diet (i.e., high-fat, high-sugar diet); Alcohol, alcohol-containing diet.

		Taxonomic level	Global R	p-value
Wild Type Mice				
WT Control (n=8)	WT Alcohol (n=8)	Phylum	0.01	0.44
		Class	0.46	<0.00*
		Order	0.45	0.01*
		Family	0.41	<0.00*
		Genus	0.363	<0.00*
Clock$^{\Delta 19}$ Mutant Mice				
Clock$^{\Delta 19}$ Control (n=8)	*Clock*$^{\Delta 19}$ Alcohol (n=8)	Phylum	0.19	0.02*
		Class	0.32	<0.00*
		Order	0.32	<0.00*
		Family	0.40	<0.00*
		Genus	0.379	<0.00*

Table 4

Alcohol significantly impacts stool microbiota community structure in both wild type and *Clock*$^{\Delta 19}$ mutant mice. Abundance of each taxon was compared between *a priori* defined comparisons using a Student's *t*-test and p-values were false discovery rate corrected for multiple comparisons. WT, wild type mice; Clk, *Clock*$^{\Delta 19}$ mutant mice; Control, alcohol-control diet; Alcohol, alcohol-containing diet; NC, no change; p_, phylum; c_, class; o_, order; f_, family; g_, genus; B, Bacteroidetes; F, Firmicutes; P, Proteobacteria; V, Verrucomicrobia..

	WT Control v WT Alcohol	Clk Control v Clk Alcohol
Class		
p_F, c_Clostridia	NC	↓ (p=0.03*)
p_F, c_Erysipelotrichi	↑ (p=0.02*)	NC
p_F, c_Bacilli	↓ (p=0.01*)	NC
Order		
P_F, c_Clostridia, o_Clostridiales	NC	↓ (p=0.03*)
p_F, c_Erysipelotrichi, o_Erysipelotrichales	↑ (p=0.02*)	NC
p_F, c_Bacilli, o_Lactobacillales	↓ (p=0.01*)	NC
Family		
p_F, c_Clostridia, o_Clostridiales, f_Clostridiaceae	NC	↓ (p=0.04*)
p_F, c_Erysipelotrichi, o_Erysipelotrichales, f_Erysipelotrichaceae	↑ (p=0.03*)	NC
p_F, c_Bacilli, o_Lactobacillales, f_Lactobacillaceae	↓ (p=0.01*)	NC
p_F, c_Clostridia, o_Clostridiales, f_Ruminococcaceae	NC	↓ (p=0.02*)
p_F, c_Clostridia, o_Clostridiales, f_Lachnospiraceae	↓ (p=0.02*)	NC
Genus		
p_F, c_Erysipelotrichi, o_Erysipelotrichales, f_Erysipelotrichaceae, g_Allobaculum	↑ (p=0.048*)	NC
p_F, c_Bacilli, o_Lactobacillales, f_Lactobacillaceae, g_Lactobacillus	↓ (p=0.01*)	NC

Table 5

Alcohol significantly impacts KEGG ortholog abundances in wild type mice. KEGG ortholog abundance was compared between groups using a Student's *t*-test and p-values were false discovery rate corrected for multiple comparisons. The number of significant between group differences was tabulated for each KEGG ortholog category. WT, wild type mice; Clk, *Clock*$^{\Delta 19}$ mutant mice; Chow, standard rodent chow diet; Control, alcohol-control diet (i.e., high-fat, high-sugar diet); Alcohol, alcohol-containing diet.

		WT Control v WT Alcohol	Clk Control v Clk Alcohol
Environmental Information Processing	Pathways Increased (%)	10 (77)	0 (0)
	Pathways Decreased (%)	0 (0)	0 (0)
Cellular Processes	Pathways Increased (%)	3 (30)	0 (0)
	Pathways Decreased (%)	1 (10)	0 (0)
Genetic Information Processing	Pathways Increased (%)	23 (88)	0 (0)
	Pathways Decreased (%)	0 (0)	0 (0)
Human Diseases	Pathways Increased (%)	10 (32)	0 (0)
	Pathways Decreased (%)	1 (3)	0 (0)
Metabolism	Pathways Increased (%)	88 (65)	0 (0)
	Pathways Decreased (%)	0 (0)	0 (0)
Organismal Systems	Pathways Increased (%)	7 (39)	0 (0)
	Pathways Decreased (%)	0 (0)	0 (0)
Unclassified	Pathways Increased (%)	20 (74)	0 (0)
	Pathways Decreased (%)	0 (0)	0 (0)

Table 6

Alcohol significantly impacts the KEGG ortholog abundances of bacterial secretion systems and lipopolysaccharide biosynthesis in wild type mice. KEGG ortholog abundance was compared between groups using a Student's *t*-test and p-values were false discovery rate corrected for multiple comparisons. The number of significant between group differences was tabulated for each KEGG ortholog category. Values are mean ± standard error of the mean. WT, wild type mice; Clk, *Clock*$^{\Delta 19}$ mutant mice; Chow, standard rodent chow diet; Control, alcohol-control diet (i.e., high-fat, high-sugar diet); Alcohol, alcohol-containing diet.

KEGG Ortholog		**WT Control (n=8)**	**WT Alcohol (n=8)**	**p-Value**
Bacterial Secretion System				
K03070	preprotein translocase subunit SecA (sec-SRP)	1701±252	3325±302	0.01
K03073	preprotein translocase subunit SecE (sec-SRP)	938±95	1621±146	0.01
K03075	preprotein translocase subunit SecG (sec-SRP)	1111±130	1931±162	0.01
K03076	preprotein translocase subunit SecY (sec-SRP)	1497±210	2979±275	0.01
K03106	signal recognition particle subunit SRP54 (sec-SRP)	1132±132	1948±162	0.01
K03110	fused signal recognition particle receptor (sec-SRP)	1080±132	1947±162	0.01
K03205	type IV secretion system protein VirD4 (type IV)	968±111	1735±156	0.01
K03217	preprotein translocase subunit YidC (sec-SRP)	1203±138	1952±162	0.02
Lipopolysaccharide Biosythesis				
K02840	UDP-D-galactose:(glucosyl) LPS alpha-1,6-D-galactosyltransferase [EC: 2.4.1.-]	25±6	6±2	0.045
K03271	phosphoheptose isomerase [EC:5.-.-.-]	642±136	1464±144	0.01
K07031	None	394±91	1068±124	0.01